**Geomechanics and Engineering**, *Vol. 40, No. 4 (2025) 229-238*
https://doi.org/10.12989/gae.2025.40.4.229


# Analysis of the water-vapor-heat coupling migration of unsaturated soil slope in seasonal frozen regions

Yongxiang Zhan[1], Mingyang Zhao*[1,2,3], Lang Qin[4], Zheng Lu[1], Gang Liu[5] and Hailin Yao[1]

[1]*State Key Laboratory of Geomechanics and Geotechnical Engineering Safety, Institute of Rock and Soil Mechanics, Chinese Academy of Sciences, Wuhan 430071, China*
[2]*University of Chinese Academy of Sciences, Beijing 100049, China*
[3]*Hubei Communications Planning and Design Institute Co., Ltd., Wuhan 430051, China*
[4]*Sichuan Chengnan Expressway Co., Ltd., Chengdu 610051, China*
[5]*CCCC Second Highway Consultants Co., Ltd., Wuhan 430056, China*

(*Received July 4, 2023, Revised January 30, 2025, Accepted January 31, 2025*)

**Abstract.** An unsaturated seasonal frozen soil slope of the Dandong-Altay highway is used as the research object. This paper is based on vapor-liquid migration and heat conduction multi-field coupling theory. The ice-water phase transition and vapor-liquid transition of water are also considered. The empirical relationship between unfrozen moisture content and ice volume fraction is introduced. A numerical model of the whole freeze-thaw process is established. The results show that: during the freezing period, the freezing depth increases faster before the temperature drops to the annual minimum temperature. Before entering the thawing period, the freezing depth is close to the maximum. After entering the thawing period, ice melting continuously absorbs heat from the frozen layer. Under the two-way action of external warming and geothermal heat, the deep freezing depth does not decrease for a long time. But it increases slowly and then decreases gradually. When the unsaturated soil slope is unfrozen, the engineering hazards of the slope caused by the migration of vapor are relatively small. After it enters the freezing state, the influence of vapor migration will increase significantly. The total volume moisture content of the frozen area is about 0.08 $m^3/m^3$ higher than without considering vapor migration.

**Keywords:** coupling water-vapor-heat migration; phase change; seasonal frozen soil region; unsaturated soil slope; VG model

## 1. Introduction

Frozen soil generally refers to soil with a temperature of less than or equal to 0°C and containing ice. Climate change, as the dominant factor in the distribution of frozen soil, affects the depth and extent of frozen soil distribution. In turn, the changes of frozen soil affect the ecological and climatic systems. Seasonal frozen soil is in the upper part of the annual temperature change layer, closer to the surface. Therefore it is more sensitive and responds more rapidly to climate change. Seasonal freezing and thawing processes affect the mechanical properties (Cheng *et al.* 2021, Jumassultan *et al.* 2021, Tang *et al.* 2020, Yilmaz and Fidan 2018) and water-energy cycles of the soil (Jiang *et al.* 2023). In the seasonal frozen environment, the slope soil is generally unsaturated. To study the characteristics of water-heat migration in slope is essential to analyze the law of water-vapor-heat coupling migration. While the traditional water-heat models (Harlan 1973, Lai *et al.* 2014, Oneill and Miller 1985, Taylor and Luthin 1978, Zhou *et al.* 2014) consider that the contribution of vapor migration to the water migration of the whole frozen soil can be ignored.

However, it is found that in regions with a high groundwater level and low moisture content, vapor migration is the main component of water migration in unsaturated seasonal frozen soil slopes. And the role of vapor migration in water-heat migration is crucial (Eigenbrod and Kennepohl 1996, Nakano *et al.* 1984). Philip and Vries (1957) first applied the local balance assumption in thermodynamics to the study of vapor migration in soil pores, investigated the migration processes of liquid water and vapor under non-isothermal conditions, and established the water-vapor-heat coupling migration equation about soil, which was the initial the PDV model. Subsequently, Some scholars completely described the water-vapor-heat coupling and confirmed the role of liquid water and vapor in the migration of thawed soil water and energy (An *et al.* 2017, Saito *et al.* 2006, Zeng *et al.* 2011). But the above models are developed for thawed soil. Zhang *et al.* (2018) established a coupling model of soil-surface-atmosphere energy balance and soil internal water-heat change considering the phase transition of liquid water and vapor, moisture convective heat transfer, and water vapor migration. Then they analyzed liquid water and vapor migration patterns in the active layer under real-field meteorological conditions by this coupling model.

As can be seen, after years of intensive research by many scholars, there are relatively more theoretical research results on the water-vapor-heat coupling migration of unsaturated soil. But most of the studies use one-dimensional models and do not consider the influence of the

*Corresponding author, MA.Eng.
E-mail: zhaomingyang2023@163.com



ISSN: 2005-307X (Print), 2092-6219 (Online)

whole process of freezing and thawing. The research results are difficult to directly serve the unsaturated soil slopes under the long-term action of the seasonal frozen environment. In this paper, for unsaturated seasonal frozen soil slopes, the relationship between matric suction and saturation is determined by van Genuchten's model (Vangenuchten 1980). We introduce an empirical relationship between unfrozen moisture content and ice volume fraction. These relations are introduced into the framework of the non-isothermal water-vapor-heat coupling PDV model considering the mass-energy balance proposed by Philip and Vries (1957). Then, by introducing the Heaviside function to characterize the ice-water phase change process during freeze-thaw, the PDV model is extended and modified. Based on numerical simulations, we reproduce the periodic process of formation, expansion, thawing, and disappearance of frozen layers on unsaturated seasonal frozen soil slopes. And we reveal the migration law of vapor and liquid water in the slope under the effect of ambient temperature and investigate the effect of vapor migration on the moisture content of the slope before and after freezing of unsaturated soil slopes.

## 2. Theory of water-vapor-heat coupling migration in unsaturated seasonal frozen soil slopes

### *2.1 Mass conservation equation*

Water migration in unsaturated frozen soil includes both liquid water and vapor migration, and both are controlled by water potential gradient and temperature gradient. The governing equation is based on the non-isothermal water-vapor-heat coupling migration model (PDV model), considering the mass-energy balance proposed by Philip and Vries (1957). It combines the Richards equation, which characterizes the migration of liquid water, and Fick's law, which characterizes the migration of vapor. And it considers the effects of matric suction gradient, gravitational gradient, and temperature gradient. The governing equation for water-vapor migration on unsaturated seasonal frozen soil slopes can be written as

$$\begin{aligned}\frac{\partial\theta}{\partial t}&=\frac{\partial\theta_l}{\partial t}+\frac{\rho_i}{\rho_w}\frac{\partial\theta_i}{\partial t}+\frac{\partial\theta_v}{\partial t}\\&=\nabla\cdot\left[K_{Lh}\nabla\left(h+z\right)+K_{LT}\nabla T+K_{vh}\nabla h+K_{vT}\nabla T\right]\end{aligned}\tag{1}$$

Where $\theta$ is the total volume moisture content, $\theta_l$ is the volume moisture content of liquid water, $\theta_i$ is the volume content of ice, $\theta_v=\rho_{vs}H_r(\theta_s-\theta_l-\theta_i)/\rho_w$ is the equivalent vapor volume moisture content; $H_r$ is the relative humidity, $H_r=\exp(hMg/RT)$; $z$ is the vertical coordinate; $h$ is the water head corresponding to the matric suction; $t$ is the time; $K_{Lh}$ is the isothermal hydraulic conductivity due to the hydraulic gradient, $K_{vh}$ is the isothermal gas conductivity, $K_{LT}$ is the non-isothermal hydraulic conductivity due to temperature gradient, $K_{vT}$ is the non-isothermal gas conductivity; $T$ is the slope soil temperature.

$$K_{Lh}=K_sS_e^{0.5}\left[1-\left(1-S_e^{1/m}\right)^m\right]^2\cdot10^{-10\theta_i}\tag{2}$$

$$K_{LT}=K_{Lh}\left(hG_{wT}\frac{1}{\gamma_0}\frac{d\gamma}{dT}\right)\tag{3}$$

$$K_{vh}=D\left(\frac{\rho_{vs}}{\rho_w}\frac{Mg}{RT}H_r\right)\tag{4}$$

$$K_{vT}=D\frac{\eta H_r}{\rho_w}\frac{d\rho_{vs}}{dT}\tag{5}$$

Where $S_e$ is the effective degree of saturation, which can be described by the van Genuchten model

$$S_e=\frac{\theta_l-\theta_r}{\theta_s-\theta_r}=\left[1+\left(-\alpha h\right)^n\right]^{-m}\tag{6}$$

Where, $a$, $n$, and $m$ are the fitting parameters of the soil water characteristic curve of unsaturated soil; $\theta_s$ is the saturated moisture content of unsaturated soil, $\theta_r$ is the residual moisture content; $K_s$ is the saturated permeability coefficient; $\gamma=(75.6\text{-}0.142T\text{-}2.38\times10^{-4}T^2)$ is the surface tension of water, $\gamma_0=71.89$ g·s$^{-2}$; $G_{wT}$ is the parameter characterizing the soil water characteristic curve influenced by temperature, generally taken as 7; $D$ is the vapor diffusivity in the soil, $D=2.12\times10^{-5}(\mathrm{T}/273.15)^2$; $M$ is the molar mass of water, $M=0.018$ kg/mol; $g$ is the acceleration of gravity; $R$ is the gas constant, $R=8.341$ J·mol$^{-1}$·K$^{-1}$;

Where $\rho_{vs}$ is the saturated vapor density, which is expressed as

$$\rho_{vs}=\frac{\exp\left(31.37-6014.79T^{-1}-7.92\times10^{-3}T\right)}{10^3\times T}\tag{7}$$

Where $\eta$ is the enhancement factor, which is expressed as

$$\eta=9.5+3\theta_l\theta_s^{-1}-8.5\left[1/\exp\left(1+2.6f_c^{-0.5}\theta_l\theta_s^{-1}\right)^4\right]\tag{8}$$

Where $f_c$ is the mass fraction of clay particles in the soil, taken as 0.05.

### *2.2 Heat conservation equation*

Considering the evaporation and condensation phase change processes in unsaturated soil together, the controlling equation for heat migration in unsaturated soil can be expressed as

$$\begin{aligned}&\mathrm{C}_p\frac{\partial T}{\partial t}+L_w\rho_w\frac{\partial\theta_v}{\partial t}-L_i\rho_i\frac{\partial\theta_i}{\partial t}\\&=\nabla\cdot\left(\lambda\nabla T\right)-C_L\nabla\cdot\left(q_lT\right)-L_w\rho_w\nabla\cdot q_v-C_v\nabla\cdot\left(q_vT\right)\end{aligned}\tag{9}$$

Where $C_p=C_n\theta_n+C_l\theta_l+C_v\theta_v+C_i\theta_i$ is total specific heat capacity of soil; $C_n$, $C_l$, $C_v$, and $C_i$ are the solid phase specific heat capacity, liquid phase specific heat capacity, gas phase specific heat capacity, and ice specific heat capacity, respectively; $\theta_n$ is the volume fraction of the solid phase, $\theta_n=1\text{-}\theta_s$; $\rho_w$ and $\rho_i$ are the density of water and ice,

respectively; $L_w$=2.501×10$^6$-2369.2$T$ is the latent heat of evaporation of water; $L_i$ is the latent heat of freezing of water, taken as 334.56 kJ/kg.

$\lambda$ is the thermal conductivity coefficient of the slope frozen soil, obtained by the exponential method (Anderson and Tice 1973)

$$\lambda=\lambda_s^{1-\theta_s}\lambda_u^{\theta_u}\lambda_i^{\theta_i}\lambda_a^{\theta_s-\theta_u-\theta_i} \tag{10}$$

Where $\lambda_s$, $\lambda_u$, $\lambda_i$ and $\lambda_a$ are the thermal conductivity coefficient of soil particles, water, ice and gas phase, respectively.

$q_l$ and $q_v$ are the liquid water flux and vapor flux, respectively, and the expressions are

$$q_l=-K_{Lh}\nabla(h+z)-K_{LT}\nabla T \tag{11}$$

$$q_v=-K_{vh}\nabla h-K_{vT}\nabla T \tag{12}$$

The liquid water content in the slope soil can be expressed by a segmental function

$$\theta_l=\begin{cases}\theta_u & T<T_0\\ \theta_w & T\geq T_0\end{cases} \tag{13}$$

Where $T_0$ is the freezing temperature.

$\theta_u$ is the unfrozen water content in unsaturated frozen soil, expressed as

$$\theta_u=(\theta_s-\theta_r)\left[1+\left(-\alpha\frac{L_iT}{gT_0}\right)^n\right]^{-m}+\theta_r \quad T<T_0 \tag{14}$$

$\theta_w$ is the liquid water content in the unfrozen region, expressed as

$$\theta_w=(\theta_s-\theta_r)\left[1+(-\alpha h)^n\right]^{-m}+\theta_r \quad T\geq T_0 \tag{15}$$

By introducing the solid-liquid ratio $B(T)$ to represent the ratio of pore ice volume to unfrozen water volume in frozen soil, the equation linking ice volume content, unfrozen water volume content, and temperature in frozen soil can be expressed as

$$\theta_i=B(T)\cdot\theta_u \tag{16}$$

$B(T)$ can be expressed as

$$B(T)=\begin{cases}\dfrac{\rho_l}{\rho_i}\left[\left(\dfrac{T}{T_0}\right)^b-1\right] & T<T_0\\ 0 & T\geq T_0\end{cases} \tag{17}$$

Where $T_0$ is the phase change point temperature, which is -0.3℃ this time.

### *2.3 Heaviside function*

The two-dimensional step-smoothed Heaviside function is introduced to characterize the ice-water transition process during freezing, as shown in Fig. 1. The expression of the Heaviside function is

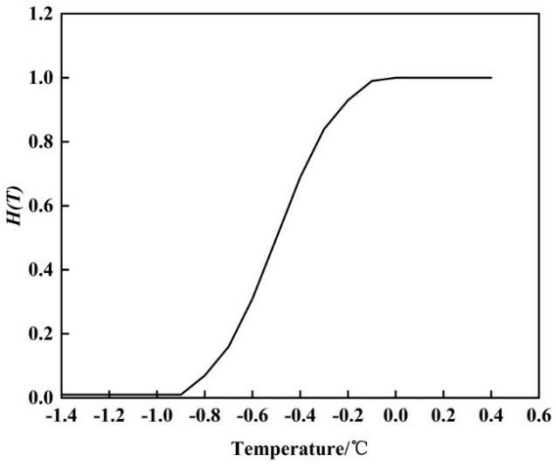


Fig. 1 Heaviside function

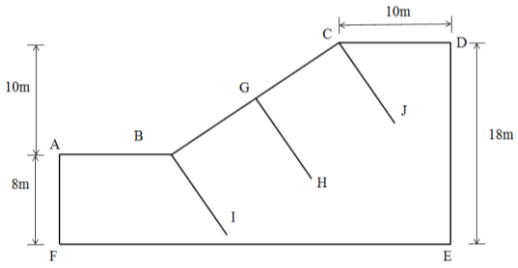


Fig. 2 Slope geometric dimension diagram

$$H(T)=flc2hs(T-T_0,dT) \tag{18}$$

Where $T$ is the slope temperature; $dT$ is the transition gap, taken as 0.3℃.

## 3. Water-vapor-heat coupling simulation of slope

### *3.1 The values of physical and mechanical parameters*

Taking a typical unsaturated soil slope on the Dandong-Altay highway as an example, the slope height is 10m, and the slope ratio is 1:1.5. The lithology is mainly silty clay. The slope geometry is shown in Fig. 2. The values of the physical and mechanical parameters of the slope are shown in Table 1.

### *3.2 Numerical algorithm and model validation*

#### *3.2.1 Numerical algorithm*

The governing Eqs. (1) and (9) can be expressed in the following uniform form:

$$d_a\frac{\partial\kappa}{\partial t}+\nabla\cdot\Gamma=f \tag{19}$$

Where $\kappa=\{\theta_l,T\}$ is the variable in the governing equation; $da$ is the damping coefficient; $\Gamma$ is the flow tensor; $f$ is the source term.

The general solution to Eq. (19) can be expressed as

Table 1 Main computational parameters

| Parameters | Value |
|---|---|
| $\rho_l$ (kg/m$^3$) | 1000 |
| $\rho_i$ (kg/m$^3$) | 918 |
| $\theta_s$ (m$^3$/m$^3$) | 0.50 |
| $\theta_r$ (m$^3$/m$^3$) | 0.01 |
| $\alpha$ (m$^{-1}$) | 0.03 |
| $n$ | 1.5 |
| $\lambda_s$ (W/m/°C) | 1.5 |
| $\lambda_u$ (W/m/°C) | 0.6 |
| $\lambda_i$ (W/m/°C) | 2.3 |
| $\lambda_a$ (W/m/°C) | 0.024 |
| $K_s$ (m/s) | $3.2\times10^{-7}$ |
| $C_n$ (MJ/m$^3$/K) | 1.92 |
| $C_l$ (MJ/m$^3$/K) | 4.18 |
| $C_i$ (MJ/m$^3$/K) | 2.1 |
| $C_v$ (MJ/m$^3$/K) | 6.3 |
| $b$ | 0.56 |

$$\left(d_a \frac{\partial \kappa}{\partial t}, \overline{\kappa}\right)_\Omega + \left(\nabla \cdot \Gamma, \overline{\kappa}\right)_\Omega = \left(f, \overline{\kappa}\right)_\Omega \tag{20}$$

Where $\overline{\kappa}$ is the considered displacement; $\Omega$ is the computational domain.

In this paper, the coefficient-type partial differential equation module in COMSOL Multiphysics is used to obtain the coefficient-type partial differential equation system with $\theta_l$ and $T$ as dependent variables. By applying certain boundary conditions and initial conditions, the water-vapor-heat coupling migration equation system is solved.

The slope surface is mainly influenced by the external ambient temperature. The periodic change of ambient temperature causes the change of slope surface temperature. According to the literature (Liu *et al.* 2007), the surface temperature can be estimated by a sine curve as follows

$$T = T_0 + A\sin\left(\frac{2\pi}{365}t + \varphi\right) \tag{21}$$

Where $T$ is the air temperature, $T_0$ is the annual average temperature of the air, a constant; $A$ is half of the annual air temperature range, a constant; $t$ is time; $\varphi$ is the initial phase.

Taking the Harbin area as an example, the daily variation of annual average temperature in Harbin from 1971 to 2000 can be expressed as

$$T = 2.35 + 20.65\sin\left(\frac{2\pi}{365}t - 5\pi/9\right) \tag{22}$$

Temperature boundary conditions: The sinusoidal temperature function shown in Eq. (22) is applied to the upper surface of slopes. The AB, BC, and CD boundaries are slope surfaces, directly expose to the air, and the pattern of temperature change is consistent with the ambient temperature. That is, the AB, BC, and CD boundaries are applied simultaneously with ambient temperature loads, and the remaining boundaries are adiabatic. The perennial geothermal temperature in this area is around 8°C. In this calculation, the initial temperature of slopes is set to be 8°C.

Moisture boundary conditions: Rainfall and evaporation are not considered. At the same time, AB, BC, and CD boundaries have no water infiltration or seepage. AF and DE are impermeable boundaries. EF is the recharge boundary. And the moisture content is set to be constant, and the saturated volume moisture content is 0.50 m$^3$/m$^3$. The initial moisture content of slopes is 0.25 m$^3$/m$^3$.

### *3.2.2 Model validation*

In order to check the solution results, this paper is based on a multifunctional soil freeze-thaw cycle device independently developed by Institute of Rock and Soil Mechanics, Chinese Academy of Sciences, as shown in Fig. 3. Freeze-thaw cycle tests on slope soil specimens were carried out. The material of sample casings is high and low temperature resistant PTFE, with a height of 150 mm and an inner diameter of 38.2 mm. A total of 6 temperature measuring holes with a diameter of 3 mm were set at intervals of 15 mm along the height of specimens in sample casings. These holes were used to place temperature sensors to monitor the changes in the internal temperature of specimens during freezing and thawing. A layer of black insulation cotton was wrapped around the outside of the sample casings to isolate the heat exchange. The inner wall of sample casings was coated with a layer of petroleum jelly to facilitate the installation and removal of specimens. Soil samples were taken on site from the unsaturated soil slope and compacted according to the natural density to make specimens with 38 mm diameter and 76 mm height. During the test, the initial temperature of the specimens was $T_0$=20°C, and the dry density of the specimens was 1.57 g/cm$^3$. The pressureless water supply method was adopted. That was, the water level was always kept flush with the bottom of the specimens during the freezing process of the specimens. After the freeze-thaw test, the total moisture content (unfrozen water and ice) at different heights of the specimens was tested using the method of moisture content measurement by stratified slicing.

During the test, the temperature at the top of specimens, i.e., the cold end, was -30°C, and the constant temperature at the warm end was 2°C. Meanwhile, the finite element model was established according to the specimen size by using the finite element software COMSOL Multiphysics. The calculated results were verified by the freezing time of 1 h, 2 h, 4 h, and 5 h for the temperature change, freezing front position, and moisture distribution.

The temperature of the soil at the freezing front of the specimens is assumed to be 0°C. Then the comparisons between the calculated freezing front position and the actual freezing front position of the specimen at different freezing times are shown in Fig. 4, where the actual freezing front of the specimens is marked with a white line. It can be seen that the calculated height and the actual height of the freezing front are both about 55 mm after freezing for 1 h.

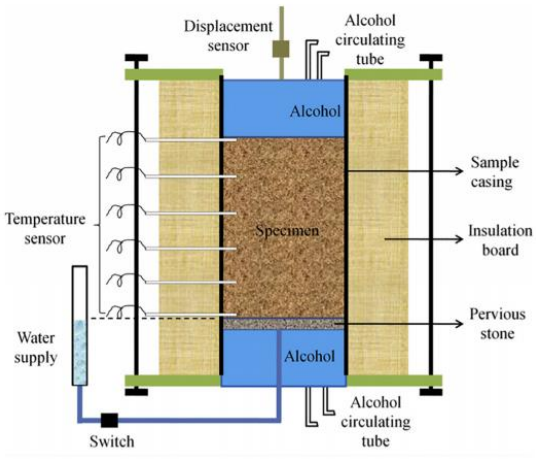


(a) Schematic diagram

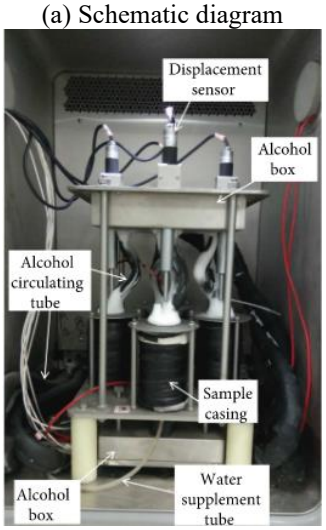


(b) Environmental chamber

Fig. 3 Apparatus for the freeze-thaw test

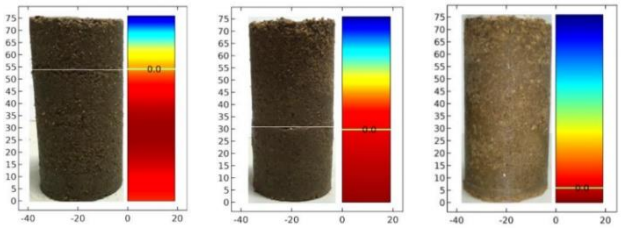

(a) t=1 h (b) t=2 h (c) t=5 h

Fig. 4 Change of freezing front during specimen freezing

After freezing for 2 h, the heights are all about 30 mm. After 5 h of freezing, the specimen has been completely frozen, and the height of the freezing front in the simulation result is about 5 mm. Therefore, the calculated position of the freezing front is basically similar to the actual position before the specimens are completely frozen. The variation of the calculated temperature and the measured temperature with the freezing time at different heights of the specimens is shown in Fig. 5. It can be seen that the changing trend of the calculated temperature and the measured temperature are consistent, and the values are relatively close, indicating that the temperature calculation results obtained by the water-vapor-heat coupling theory are credible.

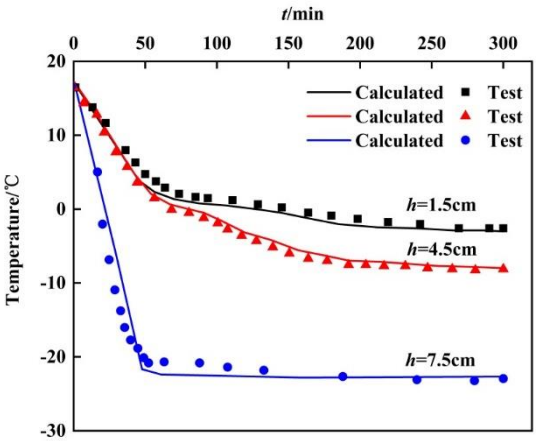


Fig. 5 Comparison between calculated temperature and test temperature of specimen

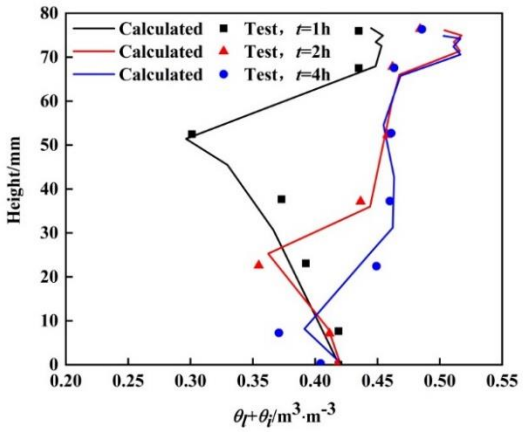


Fig. 6 Moisture distribution of specimens with different freezing time

The comparisons between the calculated value and the measured value of the total volume moisture content of the specimens with different freezing times are shown in Fig. 6.

Since the specimens are completely frozen after 5 h of freezing, only the distribution of the total volume moisture content inside the specimens at freezing times of 1 h, 2 h, and 4 h, respectively, is studied. Since the volume moisture content of equivalent vapor cannot be measured during the test, the total volume moisture content here only includes the volume moisture content of unfrozen water and ice crystals after melting into liquid water. As shown in Fig. 6, the calculated and measured moisture contents are only slightly different at the top of the specimens, while the rest of the locations are close. The overall trend of changes is basically the same, showing that the moisture contents of the upper part are higher than the lower part, and abrupt changes occur in the middle. And the calculated abrupt change locations are basically the same as the actual abrupt change locations. The abrupt change of moisture content is the freezing front. Above the front is the frozen area, and below the front is the unfrozen area. Because water migrates from the unfrozen area to the frozen area under the action of the matric potential and the temperature potential, the moisture contents of the upper part of the specimens are

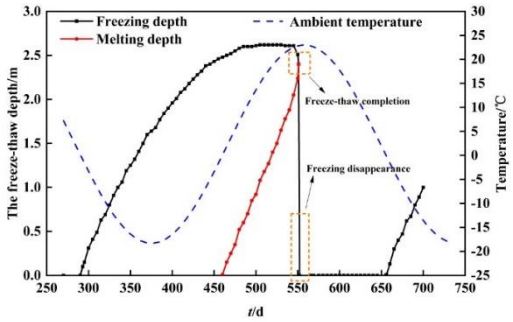


Fig. 7 Freeze-thaw depth at different times at slope top

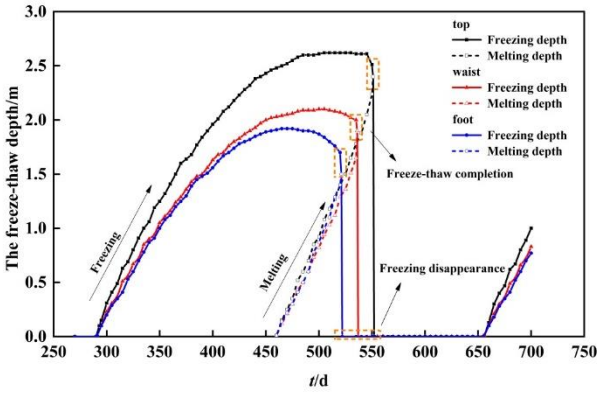


Fig. 8 Comparison of freeze-thaw depth at different locations at different times

higher than that of the lower part. The above results show that it is feasible to use the water-vapor-heat coupling theory to calculate the change in soil moisture content.

In general, the numerical calculation results can well reflect the actual temperature field of the specimen and the variation law of the moisture content distribution, which proves the rationality and correctness of the established model and parameter values.

## 4. Simulation results and analysis of unsaturated soil slopes

### *4.1 Analysis of slope temperature field*

The starting loading time starts from $t$=270 d (set as the initial state of the slope). The corresponding ambient temperature $T$=7.24℃ at this time is adapted to the initial geothermal field. The process of four seasons experienced by the unsaturated soil slope after that is studied. Three key positions of slope top, slope waist, and slope foot are selected for freeze-thaw depth analysis, and the characteristics of freeze-thaw depth change are shown in Figs. 7 and 8. The vertical coordinate is the burial depth of the dividing line between frozen soil and unfrozen soil, and the horizontal coordinate is time. Burial depth means the vertical distance from the surface of ground. When there is a dividing line at a certain moment, this burial depth is the freezing depth. When there are 2 dividing lines at a certain moment, the larger burial depth represents the freezing

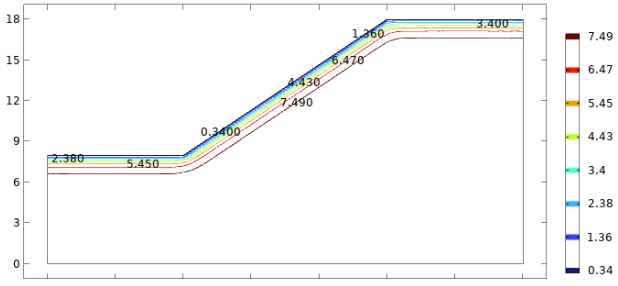


(a) t=291 d

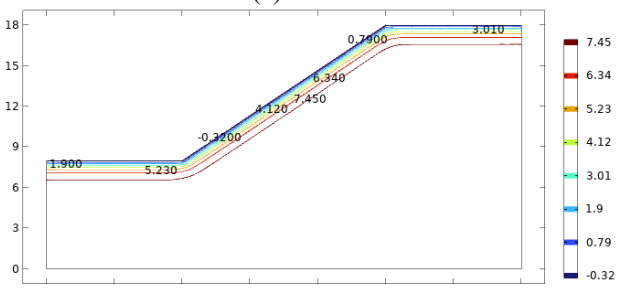


(b) t=292 d

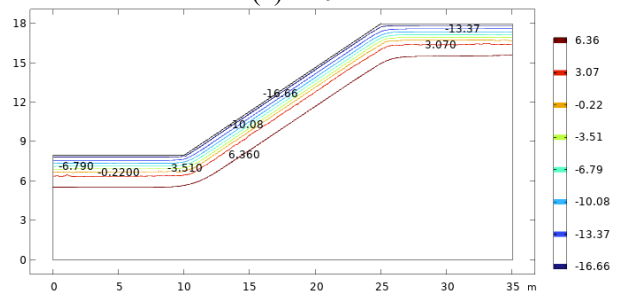


(c) t=375 d

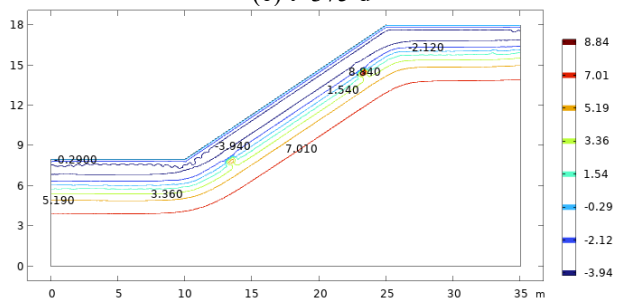


(d) t=460 d

Fig. 9 Temperature field distribution of unsaturated soil slope at typical moments

depth, and the smaller burial depth represents the melting depth of the slope after entering the melting period. The temperature field distribution of unsaturated soil slope at a typical moment is shown in Fig. 9.

It can be seen from Fig. 9 that when $t$=291 d, the ambient temperature is -0.17℃, which is already below the freezing point. Due to a certain lag in the response temperature of the slope soil, The surface layer of the slope starts to freeze and form a frozen layer at $t$=292 d. The freezing depth gradually increases as the ambient temperature decreases, and the freezing interface keeps moving inward. Until the ambient temperature drops to the lowest temperature ($t$=375 d, $T$=-18.3℃), the rate of

increase of freezing depth is faster at this stage. Subsequently, the ambient temperature gradually increases from the minimum to the freezing point, and the freezing depth still increases with the increase in ambient temperature. But the rate of increase in the freezing depth at this stage is slightly smaller than at the previous freezing stage. And the freezing depth is close to the maximum before entering the thawing period. At $t$=460 d, the ambient temperature is 0.08℃, and the slope enters the melting period. At this time, the slope begins to melt and forms a melting layer on the surface layer of the slope. The surface ice continuously absorbs heat from the frozen layer when it melts. Therefore, the freezing depth in deep depth does not decrease immediately under the two-way action of external warming and geothermal heat. Instead, it shows a small fluctuation of slow first increase and then decreases. The thawing depth gradually increases with the continuous increase of ambient temperature during the thawing period. Finally, it overlaps with the freezing depth. The freezing layer disappears. All the frozen soil on the slope melts, and the thawing period ends. In a complete freeze-thaw cycle, the freezing period is longer, and the thawing period is shorter. And the total freezing period is about twice as long as the thawing period. After that, with the cyclic ambient temperature change, the slope enters the next freeze-thaw cycle.

It can be seen from Fig. 8 that the freezing and thawing periods at the top of the slope are the longest, and the freezing depth is the largest, with a maximum freezing depth of 2.62 m. The freezing and thawing periods at the foot of the slope are the shortest, and the freezing depth is the smallest, with a maximum freezing depth of 1.92 m. The reason for this may be that the top of the slope is subject to the dual action of the original ground and the slope surface with lower temperatures, while the foot of the slope is more affected by geothermal heat.

### *4.2 Analysis of slope moisture field*

Fig. 10 shows the distribution of moisture content along the GH line for typical periods at the slope waist position before freezing (see Fig. 2 for the location of the GH line). As seen from Fig. 10, the total moisture content of the slope surface layer gradually increases as the temperature decreases before the ambient temperature drops to the freezing point. The initial moisture content of the unsaturated soil slope surface layer is low. The temperature gradient changes less, and the initial matrix potential is in equilibrium. So the migration of liquid water is extremely limited. The increase of total moisture content of the slope surface layer is mainly generated by the migration and condensation of vapor. The condensation of vapor increases the moisture in the soil and changes the moisture gradient to a certain extent. Before the temperature drops to the freezing point, there is no freezing front because the slope is not frozen. The total moisture content does not have a peak value inside the slope, and the total moisture content at the surface layer is the largest, which only increases by about 0.01 $m^3/m^3$ compared with the initial moisture content (corresponding to the state at $t$=270 d). Thus, it can be seen

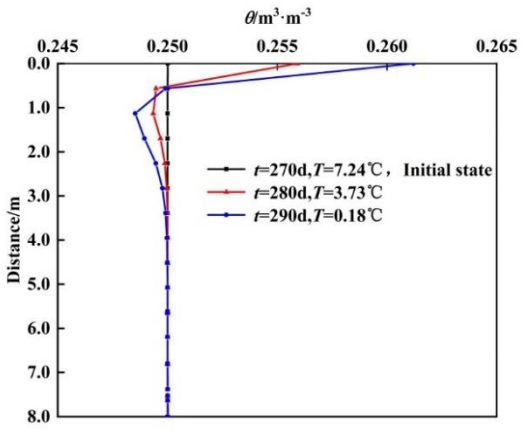


Fig. 10 Distribution of moisture content at slope waist (along the GH line) at typical times before freezing

that when the slope is in a positive temperature state, the increase of the total moisture content at the surface layer is mainly caused by the migration of vapor. However, due to the small increase, it is difficult for the shallow soil of the slope to reach saturation or near-saturation. Therefore, the engineering hazard of unsaturated soil slope caused by vapor migration is relatively small.

Figs. 11-13 show the moisture content distribution at different locations of the slope at some typical times. As shown in Figs. 11-13, the total moisture content in the negative temperature area increases significantly after the ambient temperature drops to the freezing point. The location of the sudden change of the total moisture content is the freezing front. The rapid increase of the total moisture content in the negative temperature area is due to two reasons: First, after the ambient temperature drops to the freezing point, vapor will continue to migrate to the negative temperature area and freeze into ice throughout the freezing stage. Second, the liquid water in the positive temperature area rapidly migrates from the positive temperature area to the negative temperature area under the action of the matrix potential and the temperature potential.

Most of the migrating vapor and liquid water freezes into ice near the freezing front, forming a distinct thin ice layer. A part is held back by the blocking effect of ice, resulting in a sudden change in the total moisture content near the freezing front. Only a very small part will cross the freezing front and continue to migrate to the surface frozen layer. Because ice hinders migration, the water migration in the frozen area is almost at a standstill. The total moisture content in the frozen area remains almost unchanged. As the temperature continues to drop, the freezing front gradually moves inward, and the unfrozen area is gradually eroded. The migration of vapor and liquid water repeats the above migration process.

As groundwater is located at EF, the foot of the slope is significantly affected by groundwater recharge. Therefore, the total moisture content of the unfrozen area below the frozen front at the foot of the slope is higher. The liquid water migration is more obvious. The top of the slope is the farthest away from the groundwater. The groundwater recharge is the weakest. As a result, the total moisture

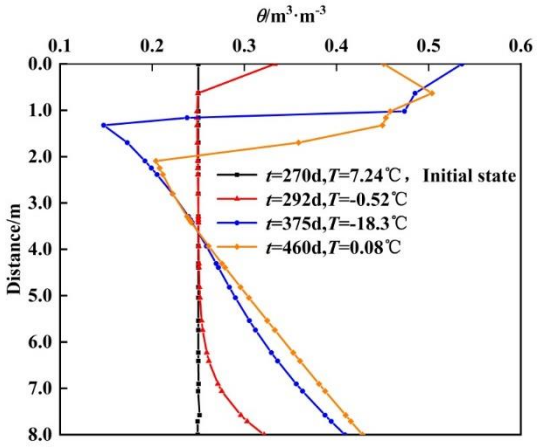


Fig. 11 Distribution of moisture content at slope foot (along the BI line) at typical times after freezing

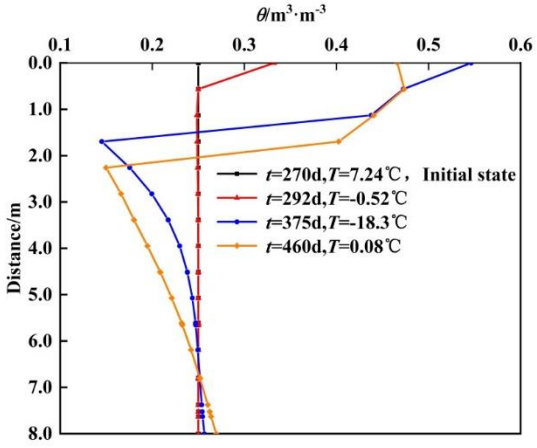


Fig. 12 Distribution of moisture content at slope waist (along the GH line) at typical times after freezing

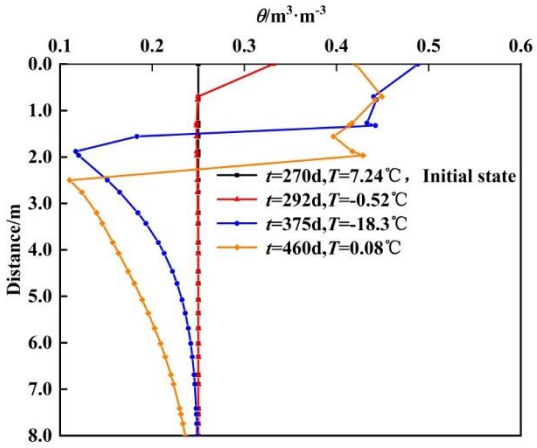


Fig. 13 Distribution of moisture content at slope top (along the CJ line) at typical times after freezing

content of the unfrozen area below the freezing front is low. However, the greater vapor migration at the top of the slope compensates for insufficient groundwater recharge. Therefore, the total moisture content of the frozen area at the top of the slope is not significantly reduced compared with that at the foot and waist of the slope.

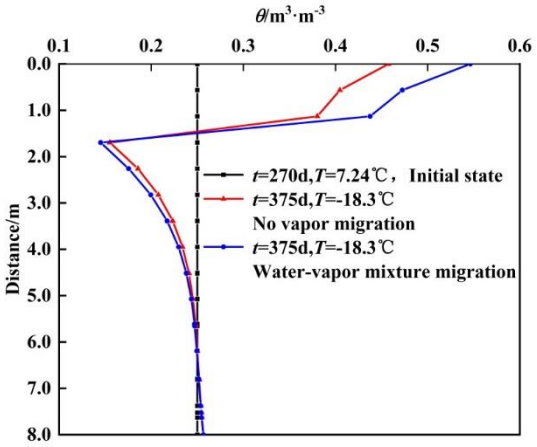


Fig. 14 Effect of vapor migration on moisture content when the ambient temperature drops to the minimum

When the slope is in the frozen state, the moisture content of the shallow layer of the slope is much higher than in the unfrozen state. The effect of vapor migration on moisture content when the ambient temperature drops to the annual minimum temperature is shown in Fig. 14. When the ambient temperature drops to the annual minimum temperature, the total volume moisture content in the frozen area without considering the migration of vapor is about 0.08 $m^3/m^3$ lower than that when considering the migration of vapor. This result shows that the absolute value of moisture increase is significant in the freezing area due to the action of vapor. It results in an average increase of about 0.08 $m^3/m^3$ in the moisture content of all soil above the freezing front. Once the spring thaw period is entered, the surface layer melts. There is still a frozen layer in the lower part of the melting layer for a relatively long period. This layer blocks the downward migration of water. So the melting water at the upper part of the freezing front will gradually collect. The moisture content of the soil at the freezing front is close to or in saturation. Thus, it may cause serious engineering diseases and should be paid enough attention.

## 5. Conclusions

Through the whole process of freeze-thaw cycle numerical simulation, the following conclusions can be obtained:

• This paper is based on the multi-field coupling theory of vapor-liquid migration and heat conduction in unsaturated seasonal frozen soil slopes. The ice-water phase transition and vapor-liquid transition of water are also considered. The empirical relationship between unfrozen moisture content and ice volume fraction is introduced. A numerical model of the whole freeze-thaw process considering water-vapor mixing migration and heat transfer is established. The coupling solution of the control equations is realized through the secondary development of COMSOL Multiphysics software. By comparing numerical solutions with laboratory freeze-thaw cycle tests, it is verified that the

established model can accurately characterize the temperature field change, water-vapor migration, and solid ice accumulation laws of frozen soil slopes.

• In the freezing period, the slope gradually freezes from outside to inside, and the freezing depth increases faster before the ambient temperature drops to the annual minimum temperature. Before entering the melting period, the freezing depth is close to the maximum. Entering the melting period, the melting depth gradually moves from outside to inside. Ice melting continuously absorbs heat from the frozen layer. Under the two-way action of external warming and geothermal heat, the deep freezing depth does not decrease for a long time. But it shows a gradual change law of increasing slowly and then decreasing gradually. In a complete freeze-thaw cycle, the freezing period is longer, and the thawing period is shorter. And the total freezing period is about twice as long as the thawing period. The freezing and thawing periods at the top of the slope are the longest, and the freezing depth is the largest. The freezing and thawing periods at the foot of the slope are the shortest, and the freezing depth is the smallest.

• When the slope is in an unfrozen state, the increase of the total moisture content of the slope surface layer is mainly generated by the migration and condensation of vapor, but the increase is small. At this time, the engineering hazard of unsaturated soil slope caused by vapor migration is relatively small.

• When the slope is in a frozen state, the total moisture content in the negative temperature area increases rapidly due to the mixing migration of water and vapor. Most of the upward-migrating vapor and liquid water freezes into ice near the freezing front, and the total moisture content abruptly changes near the freezing front. When the slope enters the freezing state, the influence of vapor migration will be significant. When the ambient temperature drops to the annual minimum temperature, the total volume moisture content in the frozen area of the slope is about 0.08 $m^3/m^3$ higher than when the vapor migration is not considered. As a result, serious engineering diseases may be caused, and enough attention should be paid to them.

## Acknowledgments

This work was supported by the National Natural Science Foundation of China (Grant Nos. 41972294, 42077262 and 42077261) and Sichuan Transportation Science and Technology Project (2021-ZL-05).

## References

An, N., Hemmati, S. and Cui, Y.J. (2017), "Numerical analysis of soil volumetric water content and temperature variations in an embankment due to soil-atmosphere interaction", *Comput. Geotech.*, **83**, 40-51. https://doi.org/10.1016/j.compgeo.2016.10.010.

Anderson, D.M. and Tice, A.R. (1973), "The unfrozen interfacial phase in frozen soil water systems", *Springer Berlin Heidelberg*, 107-125.

Cheng, S.K., Wang, Q., Fu, H.C., Wang, J.Q., Han, Y., Shen, J.J. and Lin, S. (2021), "Effect of freeze-thaw cycles on the mechanical properties and constitutive model of saline soil", *Geomech. Eng.*, **27**(4), 309-322. https://doi.org/10.12989/gae.2021.27.4.309.

Eigenbrod, K.D. and Kennepohl, G. (1996), "Moisture accumulation and pore water pressures at base of pavements", *Transport. Res. Record J. Transport. Res. Board*, **1546**(1), 151-161. https://doi.org/10.3141/1546-17.

Harlan, R.L. (1973), "Analysis of couped heat-fluid transport in partially frozen soil", *Water Resour. Res.*, **9**(5), 1314-1323. https://doi.org/10.1029/WR009i005p01314.

Jiang, X.W., Xie, H.Y., Ge, S.M., Tang, H., Tan, S.C., Wang, X.S., Wan, L. and Zeng, Y.J. (2023), "On the extinction depth of freezing-induced groundwater migration", *J. Hydrol.*, **619**. https://doi.org/10.1016/j.jhydrol.2023.129358.

Jumassultan, A., Sagidullina, N., Kim, J., Ku, T. and Moon, S.W. (2021), "Performance of cement-stabilized sand subjected to freeze-thaw cycles", *Geomech. Eng.*, **25**(1), 41-48. https://doi.org/10.12989/gae.2021.25.1.041.

Lai, Y.M., Pei, W.S., Zhang, M.Y. and Zhou, J.Z. (2014), "Study on theory model of hydro-thermal-mechanical interaction process in saturated freezing silty soil", *Int. J. Heat Mass Transfer.*, **78**, 805-819. https://doi.org/10.1016/j.ijheatmasstransfer.2014.07.035.

Liu, X.Y., Zhao, J., Shi, C. and Zhao, B. (2007), "Study on soil layer of constant temperature", *Acta Energ. Sin.*, **28**(5), 494-498 (in Chinese).

Nakano, Y., Tice, A. and Oliphant, J. (1984), "Transport of water in frozen soil IV: analysis of experimental results on the effects of ice content", *Adv. Water Resour.*, **7**(2), 58-66. https://doi.org/10.1016/0309-1708(84)90002-2.

Oneill, K. and Miller, R.D. (1985), "Exploration of a rigid ice model of frost heave", *Water Resour. Res.*, **21**(3), 281-296. https://doi.org/10.1029/WR021i003p00281.

Philip, J.R. and Vries, D.D. (1957), "Moisture movement in porous materials under temperature gradients", *T. Am. Geophys.Union*, **38**(2), 222.

Saito, H., Simunek, J. and Mohanty, B.P. (2006), "Numerical analysis of coupled water, vapor, and heat transport in the vadose zone", *Vadose Zone J*, **5**(2), 784-800. https://doi.org/10.2136/vzj2006.0007.

Tang, L.Y., Du, Y., Liu, L., Jin, L., Yang, L.J. and Li, G.Y. (2020), "Effect mechanism of unfrozen water on the frozen soil-structure interface during the freezing-thawing process", *Geomech. Eng*, **22**(3), 245-254. https://doi.org/10.12989/gae.2020.22.3.245.

Taylor, G.S. and Luthin, J.N. (1978), "Model for coupled heat and moisture transfer during soil freezing", *Can. Geotech. J.*, **15**(4), 548-555. https://doi.org/10.1139/t78-058.

Vangenuchten, M.T. (1980), "A closed-form equation for predicting the hydraulic conductivity of unsaturated soils", *Soil Sci. Soc. Am. J.*, **44**(5), 892-898. https://doi.org/10.2136/sssaj1980.03615995004400050002x.

Yilmaz, F. and Fidan, D. (2018), "Influence of freeze-thaw on strength of clayey soil stabilized with lime and perlite", *Geomech. Eng.*, **14**(3), 301-306. https://doi.org/10.12989/gae.2018.14.3.301.

Zeng, Y.J., Su, Z.B., Wan, L. and Wen, J. (2011), "A simulation analysis of the advective effect on evaporation using a two-phase heat and mass flow model", *Water Resour. Res.*, **47**, W10529. https://doi.org/10.1029/2011wr010701.

Zhang, M.L., Wen, Z., Dong, J.H., Wang, D.K., Hou, Y.D., Xue, K., Yang, X.Y. and Sun, G.D. (2018), "Coupled water-vapor-heat transport in shallow unsaturated zone of active layer in permafrost regions", *Rock. Soil. Mech.*, **39**(2), 561-570 (in Chinese).

Zhou, J.Z., Wei, C.F., Li, D.Q. and Wei, H.Z. (2014), "A moving-

pump model for water migration in unsaturated freezing soil", *Cold Reg. Sci. Technol.*, **104**, 14-22. https://doi.org/10.1016/j.coldregions.2014.04.006.

*CC*